UNIVERSIDAD TÉCNICA DE MANABÍ
Fundada en 1952

BASES DE LA CIENCIA
REVISTA CIENTÍFICA
FACULTAD DE CIENCIAS BÁSICAS

ISSN 2588-0764

Publicación Cuatrimestral. Vol. 8, No 2, Mayo/Agosto, 2023, Ecuador (p. 68-87). Edición continua
https://revistas.utm.edu.ec/index.php/Basedelaciencia/index
revista.bdlaciencia@utm.edu.ec
Universidad Técnica de Manabí
DOI: https://doi.org/10.33936/revbasdelaciencia.v8i2.5703

Ciencias Químicas

Degradation of an Antibiotic from the Fluoroquinolone Group with a New Graphitic Carbon Nitride Photocatalyst

I. Cóndor Guevara[1], A. Altamirano-Briones[2], K. Terán[3], I. Espinoza[3], L. Ramos Guerrero[4], W. Aguilar Mamani[5], C. Sandoval Pauker[6], P. Vargas Jentzsch[3], F. Muñoz Bisesti[3]

[1] Departamento de Ciencias de la Tierra y la Construcción, Universidad de las Fuerzas Armadas (ESPE), Sangolquí, Quito, Ecuador.
[2] Facultad de Ciencias Básicas, Universidad Técnica de Manabí (UTM), Av. Urbina, 130105 Portoviejo, Ecuador.
[3] Departamento de Ciencias Nucleares, Facultad de Ingeniería Química y Agroindustria, Escuela Politécnica Nacional (EPN), 170525 Quito, Ecuador.
[4] Facultad de Ingeniería y Ciencias Aplicadas, Universidad de Las Américas (UDLA), 170125, Quito, Ecuador.
[5] Departamento de Química, Facultad de Ciencias y Tecnología, Universidad Mayor de San Simón (UMSS), Cochabamba, Bolivia.
[6] Department of Chemistry and Biochemistry, University of Texas at El Paso, El Paso, Texas 79968, United States.

*Autor para correspondencia: gustavo.altamirano@utm.edu.ec

Recibido: 18-04-2023 / Aceptado: 11-08-2023 / Publicación: 31-08-2023

Editor Académico: Lenin Ruiz Davila

ABSTRACT

Ofloxacin (OFL), a fluoroquinolone, is an antibiotic found in hospital wastewater, groundwater, and other water bodies. Its occurrence in water results in several environmental problems, such as the emergence of antibiotic-resistant bacteria. This research is focused on determining the viability of removing and mineralizing OFL by photocatalysis under visible radiation with a graphitic carbon nitride photocatalyst (GCNP) synthesized from the pyrolysis of urea and calcium oxalate at 600°C. The photocatalyst was characterized by X-ray diffraction (XRD) and scanning electron microscopy (SEM). Moreover, the point of zero charge (PZC) of the photocatalyst was determined, and the adsorption isotherms were obtained. The photocatalytic activity of this new material was tested with a synthetic aqueous solution of OFL (20 mg/L) exposed to visible radiation. Three pH values (5, 7, and 10) and three doses of H_2O_2 (41.7, 83.3, and 333.2 mg/L) were considered. The achieved mineralization was evaluated through the decrease in the content of total organic carbon (TOC). The highest degradation of OFL was 23.9% after 40 min, with an initial concentration of H_2O_2 of 83.3 mg/L and a pH value of 10. It was confirmed that the reaction follows a kinetics of pseudo-first order.

Keywords: ofloxacin, water treatment, advanced oxidation processes, graphitic carbon nitride, heterogeneous photocatalysis.

Degradación de un antibiótico del grupo de las fluoroquinolonas con un nuevo fotocatalizador de nitruro de carbono grafítico

UNIVERSIDAD TÉCNICA DE MANABÍ
Fundada en 1952
BASES DE LA CIENCIA
REVISTA CIENTÍFICA
FACULTAD DE CIENCIAS BÁSICAS
ISSN 2588-0764

RESUMEN

La ofloxacina (OFL), una fluoroquinolona, es un antibiótico que se puede encontrar en aguas residuales de hospitales, aguas subterráneas y otros cuerpos de agua. Su presencia en agua resulta en muchos problemas ambientales como el surgimiento de bacterias resistentes a los antibióticos. Esta investigación se centra en determinar la viabilidad de remover y mineralizar OFL por fotocatálisis bajo radiación visible con un fotocatalizador de nitruro de carbono grafítico (GCNP) sintetizado mediante pirólisis de urea y oxalato de calcio monohidratado a 600°C. La caracterización del fotocatalizador fue llevada a cabo por difracción de rayos X y microscopía electrónica de barrido (SEM). Además, el punto de carga zero (PZC) de fotocatalizador fue determinado y se obtuvieron las isotermas de adsorción. La actividad fotocatalítica de este nuevo material fue testeada con una solución acuosa sintética de OFL (20 mg/L) expuesta a radiación visible. Tres valores de pH (5, 7 y 10) y tres dosis de H_2O_2 (41,7; 83,3 y 333,2 mg /L) fueron consideradas. La mineralización lograda fue evaluada a través del decremento en el contenido de carbono orgánico total (COT). La mayor degradación de OFL fue del 23,9% en 40 min, con una concentración inicial de H_2O_2 de 83,3 mg/L y un valor de pH de 10. Se confirmó que la degradación de OFL sigue una cinética de pseudo primer orden.

Palabras clave: ofloxacino, tratamiento de agua, procesos de oxidación avanzada, nitruro de carbono grafítico, fotocatálisis heterogénea.

Degradação de um antibiótico do grupo das fluoroquinolonas com um novo fotocatalisador de carbono nitreto gráfico.

RESUMO

A Ofloxacina (OFL), uma fluoroquinolona, é um antibiótico encontrado em águas residuais hospitalares, águas subterrâneas e outros corpos d'água. Sua presença na água resulta em vários problemas ambientais, como o surgimento de bactérias resistentes a antibióticos. Esta pesquisa tem como foco determinar a viabilidade de remover e mineralizar OFL por fotocatálise sob radiação visível com um fotocatalisador de carbono nitreto gráfico (GCNP) sintetizado a partir da pirólise de ureia e oxalato de cálcio a 600°C. O fotocatalisador foi caracterizado por difração de raios-X (XRD) e microscopia eletrônica de varredura (SEM). Além disso, o ponto de carga zero (PZC) do fotocatalisador foi determinado, e as isotermas de adsorção foram obtidas. A atividade fotocatalítica deste novo material foi testada com uma solução aquosa sintética de OFL (20 mg/L) exposta à radiação visível. Foram considerados três valores de pH (5, 7 e 10) e três doses de H_2O_2 (41,7, 83,3 e 333,2 mg/L). A mineralização alcançada foi avaliada pela diminuição do teor de carbono orgânico total (TOC). A maior degradação de OFL foi de 23,9% após 40 minutos, com uma concentração inicial de H_2O_2 de 83,3 mg/L e um valor de pH de 10. Foi confirmado que a reação segue uma cinética de pseudo-primeira ordem.

Palavras chave: ofloxacina, tratamento de água, processos de oxidação avançada, carbono nitreto gráfico, fotocatálise heterogênea..

Citación sugerida: Cóndor, I., Altamirano, A., Terán, K., Espinoza, I., Ramos, L., Aguilar, W., Sandoval, C., Vargas, P., Muñoz, F. (2023). Degradation of an Antibiotic from the Fluoroquinolone Group with a New Graphitic Carbon Nitride Photocatalyst. Revista Bases de la Ciencia, 8(2), 68-87. DOI: https://doi.org/10.33936/revbasdelaciencia.v8i2.5703

UNIVERSIDAD TÉCNICA DE MANABÍ
Fundada en 1952
BASES DE LA CIENCIA
REVISTA CIENTÍFICA
FACULTAD DE CIENCIAS BÁSICAS
ISSN 2588-0764

1. INTRODUCTION

Pharmaceutical compounds are introduced to the environment, especially through hospital wastewater, effluents from the pharmaceutical industry (Rizzo et al., 2013; Szymańska et al., 2019; Peña-Guzmán et al., 2019), and human/animal excretions (Ma et al., 2015; Chen et al., 2017; Yang et al., 2018). In this way, they can reach water bodies (i.e., rivers, lakes, reservoirs, and groundwater). Many reported studies concluded that traditional treatments are inefficient in removing these compounds from effluents (Alexander et al., 2016). Antibiotics (e.g., fluoroquinolones) generally have antimicrobial properties, which limit their biodegradation in conventional wastewater plants. The presence of antibiotics in water bodies is an important issue for ecosystems and human health because the microbiological balance in the aquatic environment can be strongly affected, leading to the selection of antibiotic-resistant bacteria (Grenni et al., 2018; Liu et al., 2018).

Ofloxacin: properties, applications, and their interaction with the environment

Ofloxacin ($C_{18}H_{20}FN_3O_4$) is an antibiotic from the group of fluoroquinolones (FQs) used to treat different types of infections, including urinary tract, skin, gonorrhea, and respiratory tract infections (Blondeau, 2004). The mechanism of action of ofloxacin (OFL) is based on the inhibition of two enzymes that interact in the synthesis of bacterial DNA, which are not present in human cells. **Figure 1** shows the structure of ofloxacin (Al-Omar, 2010). OFL has an amphoteric behavior with values of 6.1 and 8.28 for pk_{a1} and pk_{a2}, respectively (Liam et al., 2014; Van Wieren et al., 2012).

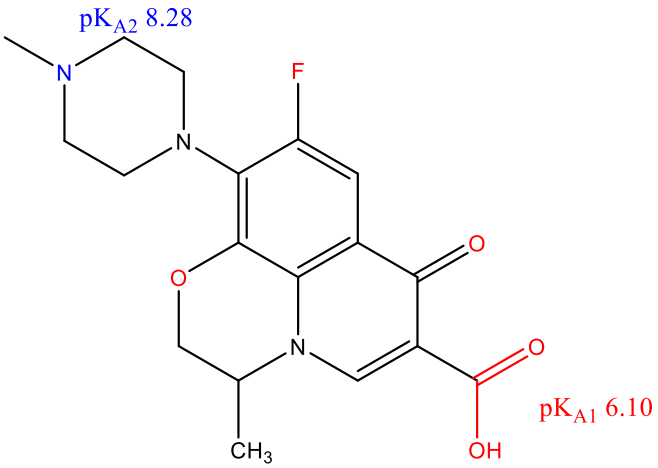

Figure 1. Chemical structure of OFL ((±)-9-fluoro-2,3-dihydro-3-methyl-10-(4-methyl-1-piperazinyl)-7-oxo-7H-pyrido[1,2,3-de][1,4]benzoxazine-6-carboxylic acid) with ionization sites

Cases of bacterial resistance to OFL have been reported in the last few years (Van Doorslaer et al., 2014; Andersson & Hughes, 2014). The problem may be associated with the presence of OFL in water in concentrations below the minimum inhibitory concentration (Allen et al., 2010; Charuaud, 2019), thus triggering an evolutionary response in surviving bacteria. These concentrations are common in wastewater where strains of antibiotic-resistant bacteria are found (Manaia et al., 2018).

Heterogeneous Photocatalysis

Advanced oxidation processes (AOPs) are a group of physicochemical treatments characterized by the generation of strong oxidizing species such as hydroxyl radicals (•OH); these processes have shown effectiveness in the removal of emerging contaminants, such as pharmaceutical residues, from water (Bayan at al., 2021; Elmolla et al., 2010; Liu et al., 2021). Even some of the last-line antibiotics, such as the antibiotics of the carbapenem family, can be degraded by processes like heterogeneous photocatalysis (Altamirano-Briones, 2020; Laverde-Cerda et al., 2020).

Heterogeneous photocatalysis occurs when a photocatalyst (e.g., semiconductors) is exposed to ultraviolet or visible radiation, and electrons of the valence band are promoted to the conduction band, generating an electron-hole pair. The "hole" in the valence band reacts with a water molecule, producing •OH radicals. These radicals are the main chemical species responsible for the degradation of organic pollutants, including the so-called emerging contaminants (Wang et al., 2022; Sandoval et al., 2017).

Graphitic carbon nitride (g-C_3N_4) is an interesting photocatalyst with advantageous characteristics such as non-toxicity, biocompatibility, and chemical/thermal resistance (Dong, 2014; Wen et al., 2017). It exhibits visible radiation activity attributable to its structure. It has a conduction band with -1.3 eV and a valence band with 1.4 eV, resulting in a bandgap of 2.7 eV. Therefore, g-C_3N_4 is highly attractive for water purification, disinfection, and organic synthesis (Chen et al., 2018; Qin et al., 2016). The nanoparticulate nature of g-C_3N_4 material poses challenges in practical applications, such as its use as a photocatalyst for water treatment, as it hinders its effective separation from water after the treatment. (Wang et al., 2018) Immobilizing g-C_3N_4 and similar photocatalysts onto inert supporting materials has been explored to facilitate the separation (Su et al., 2010).

In this work, we reported the removal of the antibiotic ofloxacin from water with a heterogeneous photocatalytic process. g-C_3N_4 was used as the photocatalyst and immobilized onto a calcium carbonate to facilitate its separation from water. The effectiveness of the heterogeneous photocatalytic

process in the removal and mineralization of ofloxacin was evaluated. In addition, the adsorption of the antibiotic on the photocatalyst was assessed.

2. MATERIALS AND METHODS

Synthesis of the graphite carbon nitride photocatalyst (GCNP)

The synthesis of g-C_3N_4 was described earlier by Liu et al. (2011). A procedure based on this report was applied; 30 g of urea, $CO(NH_2)_2$ (99.0%, Sigma-Aldrich) were mixed with 15 g of calcium oxalate monohydrate, $Ca(COO)_2H_2O$ (99%, VWR), placed in a 50 mL crucible and covered to limit the presence of oxygen during heating (condition for pyrolysis). The crucible was introduced into a muffle (A130, Vulcan), where the mixture was pyrolyzed by applying two temperature ramps: from 18 to 300 °C for 3 min and from 300 to 600°C for 40 min. Once the pyrolysis was finished, the mixture remained at room temperature for 24 h, then washed with Milli-Q® water and dried in an oven at 100°C for 3 h. For purposes of this work, this material is called “graphite carbon nitride photocatalyst (GCNP).

Characterization of the graphite carbon nitride photocatalyst

The point of zero charge (PZC) of the GCNP was determined with a method based on that described by Xie et al. (2016). 50 mL of distilled water were placed in an Erlenmeyer flask, and the pH was adjusted to a specific value by the addition of a 0.1 M HCl (37%, Riedel-de Haën) solution or a 0.1 M NaOH (98,5%, J.T. Baker) solution. Afterward, 500 mg of the GCPP was added, and the mixture was stirred with a magnetic stir bar for 24 h (speed 150 rpm). The final pH value of the solution was measured with a pH meter (HI-3220, Hanna). This procedure was applied in triplicate for different initial pH values: 4.0, 5.0, 7.0, 8.0, 9.5, and 10.5.

A Scanning Electron Microscope JSM-IT300 (Jeol) was used to obtain SEM images that allowed to obtain information on the morphology of the GCPP. In addition, an energy-dispersive X-ray analyzer (EDS) was coupled to the microscope and allowed a chemical characterization of the GCPP. For the measurement, the sample was ground to a suitable particle size.

The X-ray diffraction (XRD) measurements were carried out with an ADP PRO 2000 model X-ray diffraction system (GNR Analytical Instruments Group). The equipment operated with 30 mA and 40 kV at a 5 to 50 ° diffraction angle. The infrared spectra were recorded using a Varian 670 FT-IR

spectrometer (Agilent Technologies); measurements were performed in the 600 to 3900 cm^{-1} spectral range.

Measurement and characterization of ofloxacin samples

The concentration of ofloxacin in water was measured by high-performance liquid chromatography (HPLC). An 1120 compact LC HPLC system (Agilent Technologies) equipped with a variable wavelength UV-Vis detector (set at 294 nm) and a Zorbax Eclipse Plus C-18 column from Agilent Technologies (4.6 mm × 150 mm; 5 µm particle size) was used.

To prepare the mobile phase, 3.1 g of ammonium acetate, CH_3COONH_4 (>98%, Fluka Chemika), and 5.4 g of potassium perchlorate, $KClO_4$ (≥99%, BDM Chemicals) were dissolved in enough Milli-Q® water to obtain 1 L of solution. The pH value of the solution was adjusted to 2.2 by the slow addition of a 0.5 M fosforic acid, H_3PO_4 (85%, Fisher Scientific) solution. After the pH value was regulated, this solution was mixed with acetonitrile, CH_3CN (99.9%, Merck) in a 240:1300 ratio of acetonitrile:solution. Before use, the mobile phase was filtered through a PVDF filter with a pore size of 0.45 µm. The injection volume of both standard solutions and samples was 10 µL.

A stock solution of ofloxacin (1000 mg/L) was prepared by dissolving 0.025 g of the ofloxacin standard (99.3%, Lanfranco) in enough Milli-Q® water to obtain 25 mL of solution. Eight standard solutions (0,10; 0.50; 1.00; 5.00; 10.00; 20.00; 25.00, and 30.00 mg/L) were prepared from the stock solutions through adequate dilutions with Milli-Q® water. The injection of these standard solutions into the HPLC equipment allowed the obtention of the calibration curve. The linearity of the response was confirmed.

Total organic carbon (TOC) was measured to estimate the mineralization of OFL. Therefore, TOC measurements were performed for the water treated with the best conditions (different reaction times). TOC removals and the degradation of OFl were compared. TOC was measured according to the Standard Method 5310-B.

Adsorption of ofloxacin onto the GCNP

The time needed to reach the equilibrium concentration was determined as a first step. Adsorption tests were performed as described in the following. 10 mg of GCNP were added to 20 mL of an aqueous solution containing 20 mg/L of OFL. The mixture was magnetically stirred for 3 min at 300 rpm and then filtered through a syringe filter (PVDF, diameter of 25 mm, pore size of 0.45 µm). The concentration of OFL in the filtered solution was determined by HPLC. This procedure was repeated

for 6, 10, 20, 30, and 40 min to find the time after which the concentration of OFL does not change (equilibrium time). Also, these measurements were performed at pH 5.0 (below the PZC), 7.0, and 10.0 (above the PZC). The amount of ofloxacin adsorbed onto the GCNP was calculated with Equation S1 (Supplementary Material).

Considering the equilibrium time, adsorption isotherms were constructed as follows. 20 mg of GCNP were added to 20 mL of OFL of an aqueous solution containing 20 mg/L of OFL and stirred at 300 rpm for the established equilibrium time. This process was then repeated for different amounts of GCNP: 30, 40, 50, and 60 mg.

The correlation of the results of the adsorption test with the models of Langmuir and Freundlich was evaluated. The linear forms of the equations of Langmuir and Freundlich are shown in Equations S2 and S3 (Supplementary Material).

Heterogeneous photocatalytic degradation of ofloxacin

The removal of OFL from water was carried out with a heterogeneous photocatalytic process. An adapted procedure to that described by Altamirano Briones et al. (2020) was applied with the GCNP photocatalyst under visible radiation. The experimental system used to test the removal of OFL is shown in **Figure S1** (Supplementary Material). Degradation tests were performed in Petri dishes; 20 mL of an aqueous solution containing 20 mg/L of OFL and 10 mg of the GCNP were added to a Petri dish and maintained constantly stirred (300 rpm). The photocatalytic reaction was carried out with visible radiation provided by a 35 W xenon lamp (λ_{max} = 481 nm) placed at a distance of 8 cm from the reacting mixture. First, the mixture was kept in darkness (the lamp was off) for enough time to ensure that adsorption equilibrium was reached, and then the lamp was switched on. Since the volume of the solution was small (20 mL), individual experiments were performed to determine the degradation of OFL at different times (1, 3, 6, 8, 10, 20, 30, and 40 min). After each experiment, the solution was filtered through a syringe filter (PVDF, diameter of 25 mm, pore size of 0.45 µm), and then the concentration of OFL was measured by HPLC. Three levels of pH values were tested: 5.0, 7.0, and 10.0. These values correspond to a level below the first pK_a of OFL, the pH value of the aqueous solution of the antibiotic without the addition of any chemical species, and a value above the PZC of the GCNP, respectively. The pH value of OFL solutions was adjusted by adding 0.1 M NaOH or 0.1 M HCl, depending on the desired final pH.

From these first experiments, the pH value that allowed the higher degradation of OFL was selected. Considering this pH value, experiments with the addition of hydrogen peroxide (H_2O_2) were carried out. The experiments with the photocatalyst were repeated, adding enough solution of H_2O_2 (30% w/w, Scharlau) to obtain initial concentrations of 41.7, 83.3, and 333.2 mg/L. Again, for each concentration of H_2O_2, the remaining concentration of OFL at different times (1, 3, 6, 8, 10, 20, 30, and 40 min) was determined. Since the presence of H_2O_2 can interfere with the measurement of OFL, the remanent H_2O_2 in the solutions was eliminated by increasing the pH value up to 12 with a 0.5 M NaOH solution and, afterward, decreasing the pH value to 7 (pH value of the aqueous solutions that is injected into the HPLC equipment).

The Petri dish (reactor) was maintained at a stable temperature (around 20°C) using a continuous water flow system. The temperature of the solutions was monitored throughout the process, and water evaporation was also carefully controlled.

3. RESULTS AND DISCUSSION

Synthesis and characterization of the photocatalyst

Figure 2 shows the resulting GCNP after the washing, sonication, and drying processes. The resulting solid is a granolous material with a yellowish coloration, which suggests the presence of g-C_3N_4 (Picho-Chillán et al., 2019). The yield of the pyrolysis reaction to produce GCNP was about 3.7% by weight, considering the mass of reagents and precursors.

Figure 2. Synthesized photocatalys of g-C_3N_4 (GCNP).

ISSN 2588-0764

The presence of the photoactive species g-C_3N_4 in the GCNP material can be further confirmed by a naked-eye inspection of the color and appearance of samples of pyrolyzed calcium oxalate monohydrate, pure g-C_3N_4, and a GCNP sample (see **Figure 3**). The pyrolyzed calcium oxalate monohydrate was transformed into $CaCO_3$ (see also XRD and FTIR results) and presented a greyish color, possibly due to certain amounts of carbon that may have been formed during heating in an oxygen-poor atmosphere. This transformation to $CaCO_3$ was expected because, according to Lewis et al. (2021), when calcium oxalate monohydrate is subjected to a temperature between 450 and 700 °C, $CaCO_3$ is produced. Compared to bare g-C_3N_4 and pyrolyzed calcium oxalate, GCNP samples have a larger particle size and coloration, suggesting the formation of a different material (see also SEM-EDS and FTIR XRD characterization).

Figure 3. Samples of a) pyrolyzed monohydrate calcium oxalate ($CaCO_3$), b) GCNP, c) pyrolyzed urea (g-C_3N_4).

SEM-EDS characterization of the photocatalyst

SEM analysis confirmed the deposition of g-C_3N_4 onto the surface of the pyrolized calcium oxalate particles. As shown in the image at 13000x magnification (**Figure 4b**), small particles of nanoparticulated size (<100 nm), presumably g-C_3N_4, are deposited onto the surface of $CaCO_3$ particles (see below) with a size between 2 and 5 μm (**Figure 4a**).

UNIVERSIDAD TÉCNICA DE MANABÍ
Fundada en 1952
BASES DE LA CIENCIA
REVISTA CIENTÍFICA
FACULTAD DE CIENCIAS BÁSICAS
ISSN 2588-0764

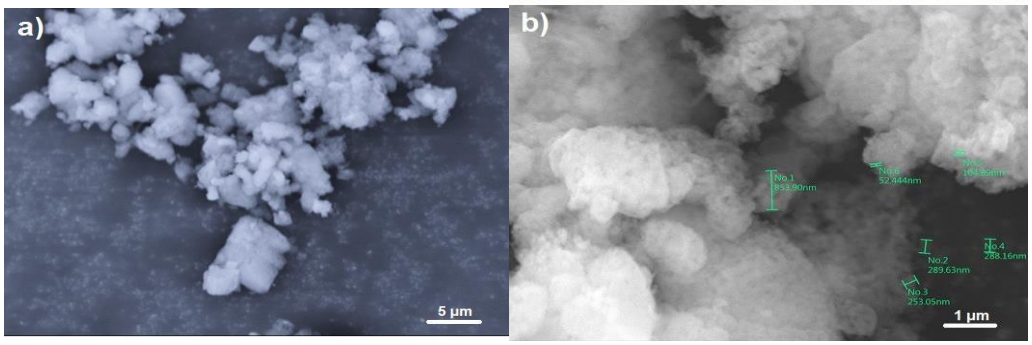

Figure 4. SEM image of photocatalyst (GCNP): a) x2700, y b) x13000

Figure 5 shows the chemical mapping of the GCNP, which was obtained by EDS analysis. This analysis confirmed that the elementary composition of the material is carbon (C), oxygen (O), calcium (Ca), and nitrogen (N). The purple dots in **Figures 5a** and **5c** confirm the homogeneous distribution of g-C_3N_4 on the surface of $CaCO_3$ support. Both $CaCO_3$ and g-C_3N_4 supply carbon. Nevertheless, during the pyrolysis of calcium oxalate monohydrate, the formation of carbon cannot be ruled out. Initially, the removal of hydration water occurs, followed by the transformation of calcium oxalate into $CaCO_3$, probably accompanied by the release of carbon monoxide (Ismael, 2020). However, it is plausible that the reaction conditions, marked by a limited presence of oxygen, facilitated the generation of carbon. This carbon may account for the observed greyish color in $CaCO_3$, which is conventionally white in its pure form.

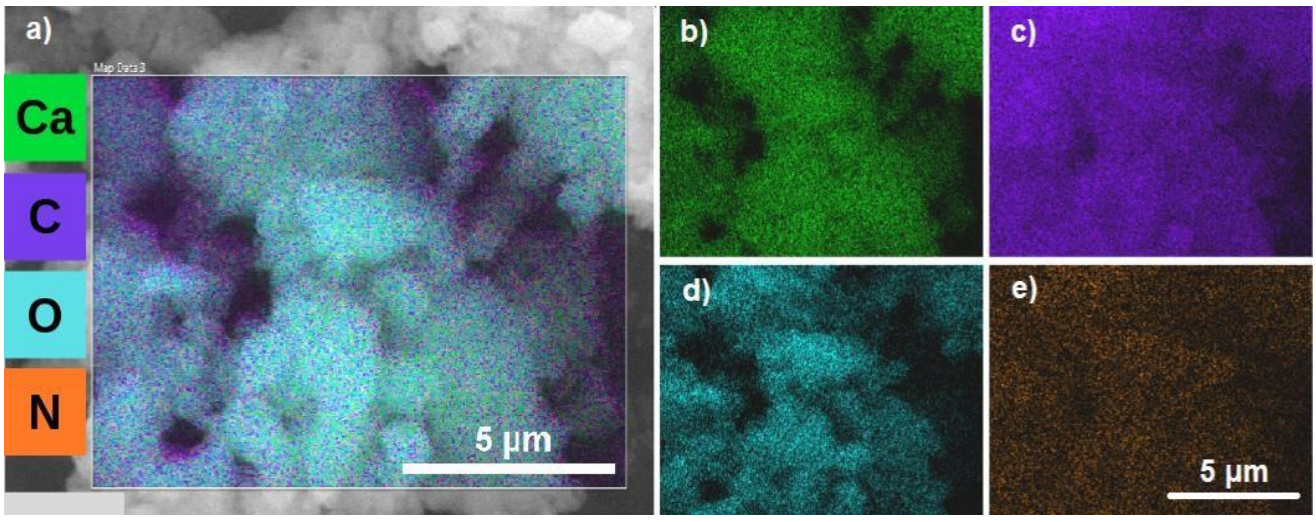

Figure 5. EDS analysis of the GCNP: a) chemical mapping, b) calcium, c) carbon, d) oxygen, and e) nitrogen.

ISSN 2588-0764

FTIR-XRD characterization of the photocatalyst

The XRD pattern of the GCNP is shown in **Figure 6**. The diffraction peaks observed in the pattern agree with the characteristic signals of $CaCO_3$ (Ni & Ratner, 2008). However, the typical signal of g-C_3N_4 near 27.5° is not distinguished, possibly attributed to the lower amount of g-C_3N_4 in the material than $CaCO_3$.

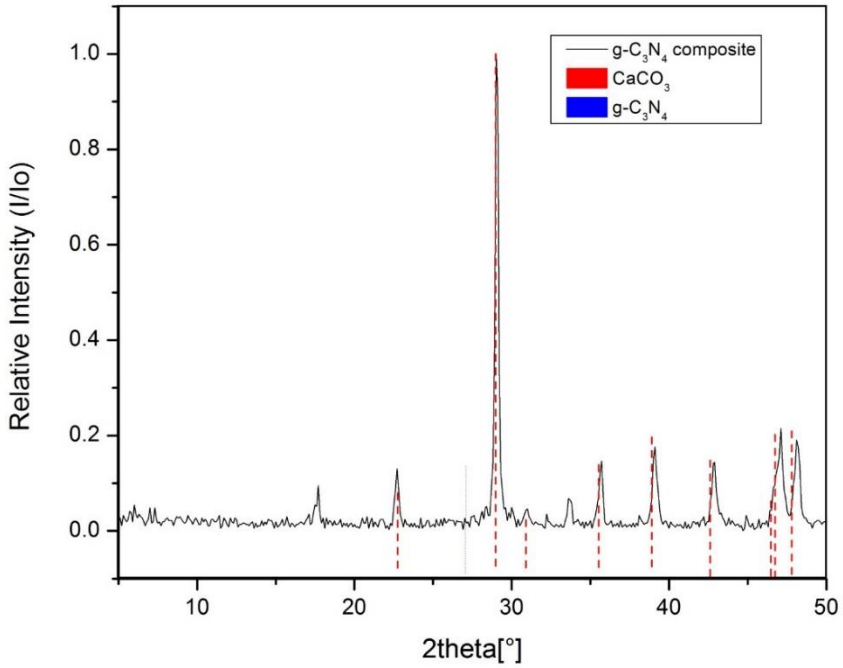

Figure 6. X-ray diffraction pattern of the photocatalyst.

FTIR measurements were performed for the $CaCO_3$, g-C_3N_4, and GCNP to corroborate the composition of the GCNP. As can be seen in **Figure 7**, the infrared spectrum of the GCNP shows the characteristic bands of $CaCO_3$ at wavenumbers of 1404, 873, and 713 cm^{-1}, which can be assigned to the asymmetric stretching of CO_3, the asymmetric bending of CO_3 and the symmetric bending CO_3 deformation, respectively (Yu et al., 2018). Three weak signals at 1636, 1565, and 1255 cm^{-1} are also observed in GCNP and are typical of g-C_3N_4 aromatic heterocycles (Cui et al., 2012). The fact that weak g-C_3N_4 bands are observed compared to the $CaCO_3$ bands in the IR spectrum of the GCNP suggests that $CaCO_3$ could be the main component in the photocatalyst.

ISSN 2588-0764

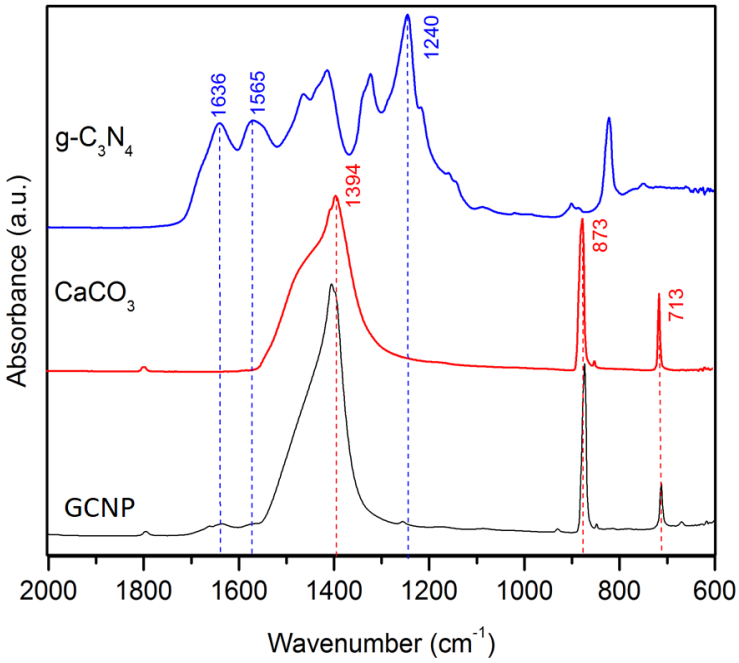

Figure 7. Infrared spectra of pure g-C_3N_4, $CaCO_3$, and GCNP. Dashed lines indicate the characteristic bands of $CaCO_3$ (red) and g-C_3N_4 (blue).

PZC and adsorption isotherms

The PZC of the GCNP material was measured using the methodology described in Section 2. A plot of the initial pH of the aqueous solutions before depression (x-axis) vs. the final pH after the 24-hour depression time had elapsed (y-axis) was prepared (see raw data in **Table S1** – Supplementary Material). The point where both curves intersected corresponded to the PZC of the material (Kosmulski, 2018). As shown in **Figure 8**, the PZC value of the GCNP is 8.3, which agrees with the PZC of $CaCO_3$ (~ 8.0), a major component of GCNP. The PZC of the GCNP indicates the pH value at which the sum of the positive charges and the sum of the negative charges on the photocatalyst surface are equal, giving it a neutral charge (Xie et al., 2016). The catalyst surface is negatively charged at pH values above the PZC and positively charged at pH values below the PZC (Kong., 2017).

Adsorption studies were conducted at the natural pH of OFL in the aqueous phase (pH = 7.0) to determine the adsorption behavior of GCNP towards OFL. At this specific pH, the concentration of OFL decreased during the first 20 min of stirring, reaching the adsorption equilibrium. At these experimental conditions (pH = 7, initial OFL concentration = 20 mg/L, and GCNP loading = 10 mg), the removal of OFL achieved by adsorption was 9.91%.

UNIVERSIDAD TÉCNICA DE MANABÍ
Fundada en 1952
BASES DE LA CIENCIA
REVISTA CIENTÍFICA
FACULTAD DE CIENCIAS BÁSICAS
ISSN 2588-0764

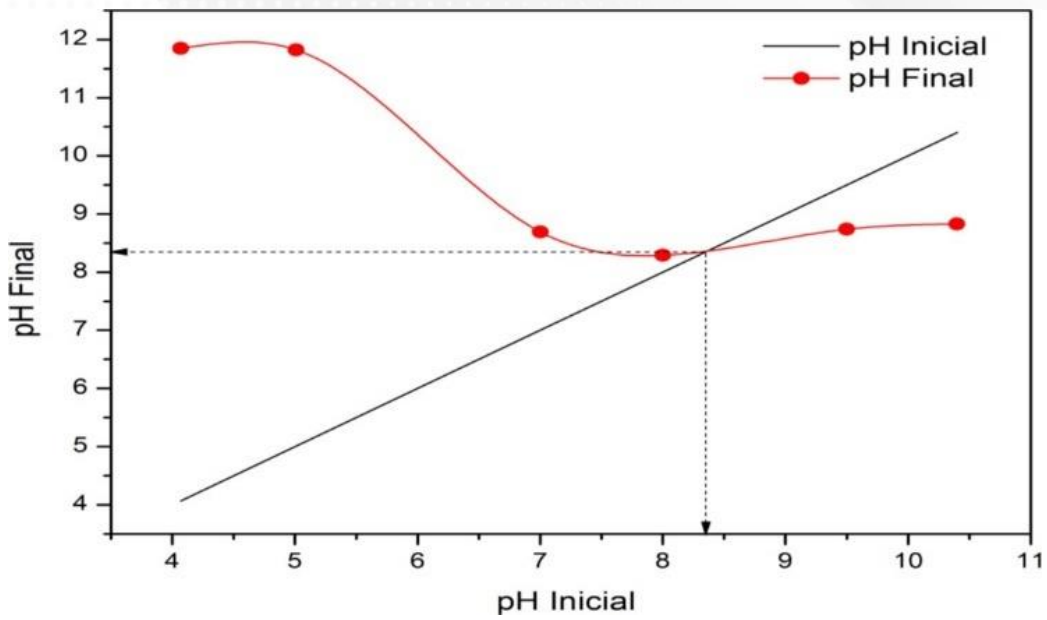

Figure 8. Plot of the final pH vs. initial pH of OFL solutions equilibrated with GCNP. The intersection of both lines indicates the point of zero charge (PZC) of the GCNP.

Conversely, at pH = 10, the adsorption equilibrium is reached after 10 min, achieving a 10.95% removal of OFL. The low removal of OFL by adsorption can be explained by electrostatics. It is known that ofloxacin may be in the form of zwitterionic species at pH = 7 and anionic species at pH = 10. (Van Wieren, 2012) Since the PZC of GCNP is 8.3, it is expected that at pH = 10.0, the repulsion between the negatively charged surface of the photocatalyst and OFL anions will hinder the adsorption. At pH = 7.0, the positively charged surface may only interact with the deprotonated carboxylate group of OFL, obliging OFL to adapt a specific configuration onto the surface of the GCNP, which may heavily depend on the presence of particular functional groups on the material. Furthermore, the adsorption data were fitted to Langmuir (r^2 = 0.83 at pH = 10) and Freunlich (r^2 = 0.98) isotherm models, and a better fit was obtained for the latter (K_F = 0.44 L/mg and 1/n = 0.74). The results of the adsorption tests are detailed in **Table S2** (Supplementary Material).

Evaluation of the activity of the photocatalyst: Oxidation of ofloxacin

Figure 9 presents a plot showing the decrement in the concentration of OFL as a function of the reaction time, at different pH values. After 40 min of reaction, the degradation of OFL achieved at a pH value of 7.0 is similar to the degradation achieved at a pH value of 10.0; the degradation percentages were 11.85 and 11.72%, respectively. The degradation achieved at a pH value of 5.0 was 8.78%. The relatively low degradation percentages that were obtained with these treatments may be

attributed to the limited photocatalytic capacity of GCNP. It may be possible that the OFL interacts with the GCNP in areas where $CaCO_3$ is present instead of g-C_3N_4 (Su et al., 2022). This also implies that there was a low quantity of g-C_3N_4 deposited onto the $CaCO_3$. Nevertheless, an advantage of GCNP was its easy separation from water when the treatment was complete. When the stirring system stopped, the GCNP sedimented and water was effectively separated by decantation. The amount of g-C_3N_4 deposited onto the $CaCO_3$ could be improved by modifying certain variables in the preparative procedure of the GCNP. For example, some changes in temperature ramps as well as the potential inclusion of reprocessing stages can be tested.

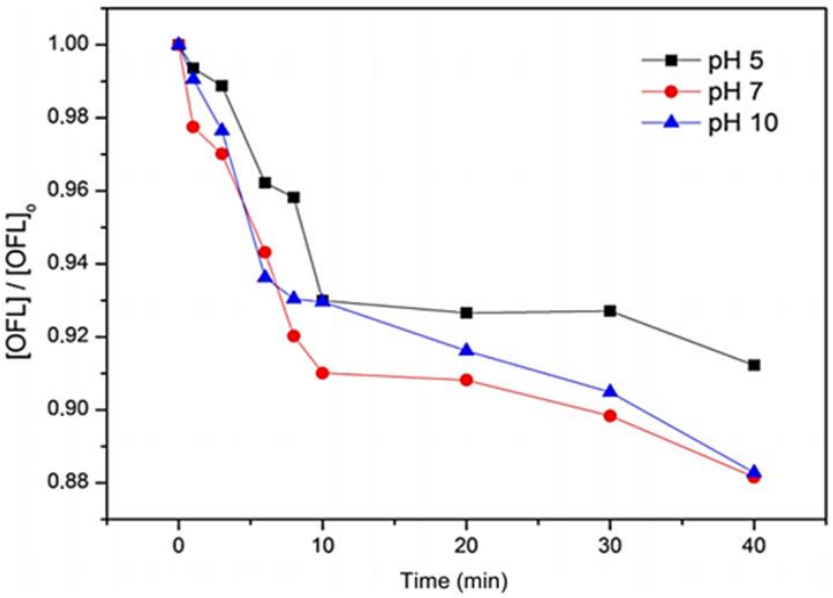

Figure 9. Plot of the degradation of OFL in time by heterogeneous photocatalysis using the GCNP, evaluated at different pH values. $[OFL]_0$ and [OFL] represent the initial concentration of OFL and the concentration of OFL at a specific time, respectively.

In order to separate the effect of the adsorption of OFL onto the GCNP from the degradation of OFL due to the heterogeneous photocatalytic process, the mixture consisting of the solution of OFL and the GCNP was first stirred in the absence of visible radiation (lamp off), this for enough time to reach the adsorption equilibrium. Afterward, the lamp was turned on to start the photocatalytic process. Therefore, it was established that the initial concentration of OFL in the aqueous solution ($[OFL]_0$) was the concentration corresponding to adsorption equilibrium. Starting from this concentration of OFL, the concentration of the antibiotic ([OFL]) decreased as the photocatalytic process progressed, as shown in **Figure 9**.

Effect of the addition of hydrogen peroxide in the heterogeneous photocatalytic process

The degradation of OFL due to the heterogeneous photocatalytic process can be improved by the addition of H_2O_2 since this compound is also a precursor of •OH. From the experiments without H_2O_2, it was demonstrated that treatments that took place at pH values of 7 and 10 allowed the highest degradation percentages. From a technical point of view, both pH values could be selected for the treatment. On one hand, a pH value of 7 for the treatment would be appropriate since this is the natural pH of the aqueous solution of OFL and no chemicals (neither acids nor bases) must be added to adjust the pH value. On the other hand, a pH value of 10, as a first approach, seems appropriate since the pH value would be above the PZC of the GCNP, thus facilitating the adsorption OFL onto the photocatalyst. If the adsorption on the photocatalyst increases, the photocatalytic process also improves.

Taking into consideration the mentioned considerations, the degradation tests were carried out with the addition of H_2O_2 at pH values of 7 and 10. The solution of OFL was equilibrated with the GCNP, then the lamp was switched on and almost immediately the concentrated solution of H_2O_2 was added to the mixture. The tested concentrations of H_2O_2 were: 41.7; 83.3 and 333.2 mg/L, which were established based on the stoichiometric (theoretical) amounts necessary to mineralize the OFL. **Figure 10**, presents a plot showing the decrement in the concentration of OFL as a function of the reaction time, at different pH values and concentrations of H_2O_2. The values of the apparent rate constant of the degradation of OFL, using different concentrations of H_2O_2 and applying the pH values of 7 and 10, are summarized in **Table S3** (Supplementary Material).

The variation in the degree of mineralization of OFL in time for the best conditions of treatment (pH = 10 and initial concentration of H_2O_2 of 83.3 mg/L) is shown in the plot of **Figure 11**. As expected, the mineralization is lower than the degradation of OFL. The degradation of OFL, and any other organic compound, implies the decrement in the concentration of OFL and the formation of other organic compounds that also contribute to the content of total organic carbon (TOC) of the solution. OFL is, progressively, in lower concentration as time passes, however, only a fraction of the degradation products of OFL suffer further degradation/oxidation reactions that finally lead to total mineralization (i.e., the total evolution of the organic compound to most oxidated and stable inorganic forms like CO_2, NO_3^-, F^- and H_2O).

ISSN 2588-0764

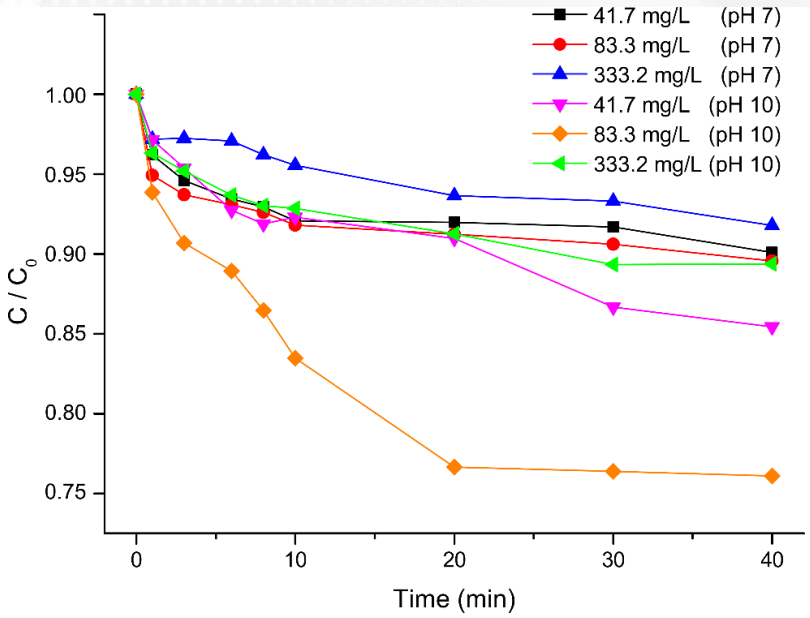

Figure 10. Plot of the degradation of OFL in time by heterogeneous photocatalysis using the GCNP, evaluated at different pH values and with different concentrations of H_2O_2. $[OFL]_0$ and [OFL] represent the initial concentration of OFL and the concentration of OFL at a specific time, respectively.

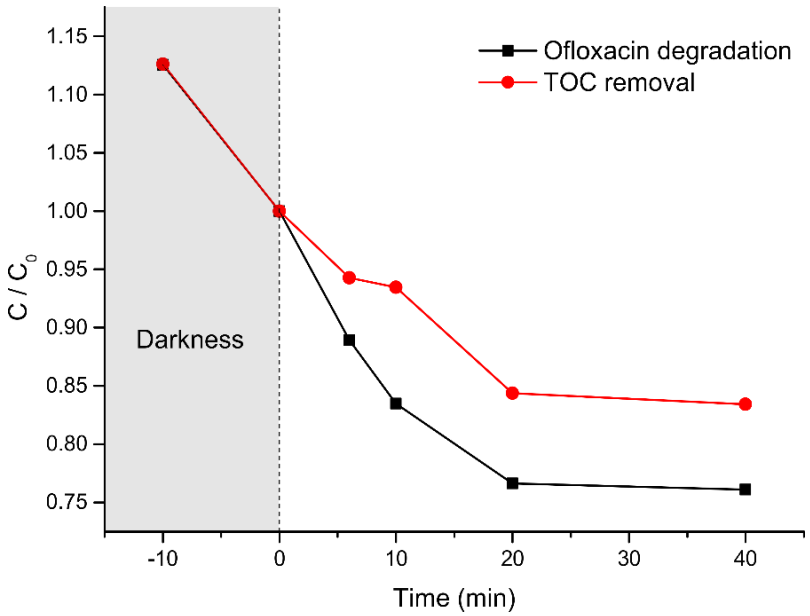

Figure 11. Plot of the degradation and mineralization (expressed in terms of total organic carbon, TOC) of OFL in time by heterogeneous photocatalysis using the GCNP, evaluated at pH = 10 and using an initial concentration of H_2O_2 of 83.3 mg/L. C_0 and C represent the initial concentration and the concentration at a specific time for both OFL and TOC, respectively.

As is possible to see in the plot of **Figure 11,** 11.20% of the COT was removed during the initial 10 min required to equilibrate the solution of OFL with the GCNP. An additional removal of 16.57% of COT was achieved due to the heterogeneous photocatalytic process. Therefore, based on the composition of the GCNP and the perspective that further improvements in the amount of g-C_3N_4 that can be deposited and retained onto the particles of $CaCO_3$, is reasonable to consider promising this kind of photocatalysts.

4. CONCLUSIONS

The new photocatalyst exhibited photocatalytic activity with visible radiation. For this reason, it could be used for the removal of OFL from water in treatment systems based on heterogeneous photocatalysis.

The point of zero charge (PZC) of the GCNP was 8.35 (i.e., above this pH value, the photocatalyst is negatively charged, while above it, it is positively charged). This result is relevant since suggests that the adsorption of OFL is favored at pH values as high as 10. Tests carried out at this pH value suggest that adsorption plays a remarkable role in the removal of OFL.

In the photocatalyst (GCNP), the graphitic carbon nitride was supported onto calcium carbonate particles (sizes around 2 and 5 µm). The composition of this material was confirmed by XRD and SEM-EDS measurements. It was possible to verify the presence of carbon, calcium, nitrogen, and hydrogen in the photocatalyst. The adsorption of OFL showed a better fit to the Freundlich isotherm than to the Langmuir isotherm.

OFL can be degraded in a heterogeneous photocatalytic process with a photocatalyst based on graphitic carbon nitride. The highest degradation of OFL (23.90%) was observed when the treatment occurred with a pH value of 10 and an initial concentration of H_2O_2 of 83.3 mg/L. Adsorption on the GCNP allowed the removal of 11.20%, thus being an important contributor to the elimination of the antibiotic from water. Although the achieved degradation and mineralization could be considered low, there is room for improvement. Future works should focus on increasing the amount of graphitic carbon nitride deposited on the surface of the supporting material. In this way, the degradation of OFL (and a variety of other pharmaceuticals) could be can be accomplished efficiently.

5. DECLARACIÓN DE CONFLICTO DE INTERÉS DE LOS AUTORES

Los autores declaran no tener conflicto de intereses.

6. REFERENCES

Alexander, J., Knopp, G., Dötsch, A., Wieland, A., & Schwartz, T. (2016). Ozone treatment of conditioned wastewater selects antibiotic resistance genes, opportunistic bacteria, and induce strong population shifts. Science of the Total Environment, 559, 103-112. doi:10.1016/j.scitotenv.2016.03.154.

Allen, H. K., Donato, J., Wang, H. H., Cloud-Hansen, K. A., Davies, J., & Handelsman, J. (2010). Call of the wild: antibiotic resistance genes in natural environments. Nature reviews microbiology, 8(4), 251-259. https://doi.org/10.1038/nrmicro2312

Al-Omar, M. A. (2009). Ofloxacin. In Profiles of drug substances, excipients and related methodology (Vol. 34, pp. 265-298). Academic Press. https://doi.org/10.1016/S1871-5125(09)34006-6

Andersson, D. I., & Hughes, D. (2014). Microbiological effects of sublethal levels of antibiotics. Nature Reviews Microbiology, 12(7), 465-478. https://doi.org/10.1038/nrmicro3270

Altamirano Briones, A., Cóndor Guevara, I., Mena, D., Espinoza, I., Sandoval-Pauker, C., Ramos Guerrero, L., ... & Muñoz Bisesti, F. (2020). Degradation of meropenem by heterogeneous photocatalysis using TiO2/fiberglass substrates. Catalysts, 10(3), 344. https://doi.org/10.3390/catal10030344

Bayan, E. M., Pustovaya, L. E., & Volkova, M. G. (2021). Recent advances in TiO2-based materials for photocatalytic degradation of antibiotics in aqueous systems. Environmental Technology & Innovation, 24, 101822. https://doi.org/10.1016/j.eti.2021.101822.

Blondeau, J. M. (2004). Fluoroquinolones: mechanism of action, classification, and development of resistance. Survey of ophthalmology, 49(2), S73-S78. https://doi.org/10.1016/j.survophthal.2004.01.005.

Charuaud, L., Jarde, E., Jaffrezic, A., Thomas, M. F., & Le Bot, B. (2019). Veterinary pharmaceutical residues from natural water to tap water: sales, occurrence and fate. Journal of hazardous materials, 361, 169-186. https://doi.org/10.1016/j.jhazmat.2018.08.075.

Chen, L., Lang, H., Liu, F., Jin, S., & Yan, T. (2018). Presence of antibiotics in shallow groundwater in the northern and southwestern regions of China. Groundwater, 56(3), 451-457. https://doi.org/10.1111/gwat.12596

Chen, Y., Lu, W., Wang, X., & Chen, W. (2018). Graphitic carbon nitride embedded in hot-melt adhesive polyester and hydrophilic cellulose blend fibers for the efficient elimination of antibiotics under solar irradiation. Applied Surface Science, 453, 110-119. https://doi.org/10.1016/j.apsusc.2018.04.188.

Cui, Y., Ding, Z., Liu, P., Antonietti, M., Fu, X., & Wang, X. (2012). Metal-free activation of H2O2 by g-C3N4 under visible light irradiation for the degradation of organic pollutants. Physical Chemistry Chemical Physics, 14(4), 1455-1462. DOIhttps://doi.org/10.1039/C1CP22820J

Dong, G., Zhang, Y., Pan, Q., & Qiu, J. (2014). A fantastic graphitic carbon nitride (g-C3N4) material: electronic structure, photocatalytic and photoelectronic properties. Journal of Photochemistry and Photobiology C: Photochemistry Reviews, 20, 33-50. https://doi.org/10.1016/j.jphotochemrev.2014.04.002.

Elmolla, E. S., & Chaudhuri, M. (2010). Photocatalytic degradation of amoxicillin, ampicillin and cloxacillin antibiotics in aqueous solution using UV/TiO2 and UV/H2O2/TiO2 photocatalysis. Desalination, 252(1-3),46-52. https://doi.org/10.1016/j.desal.2009.11.003.

Fallah, Z., Zare, E. N., Ghomi, M., Ahmadijokani, F., Amini, M., Tajbakhsh, M., ... & Varma, R. S. (2021). Toxicity and remediation of pharmaceuticals and pesticides using metal oxides and carbon nanomaterials. Chemosphere, 275, 130055. https://doi.org/10.1016/j.psep.2017.05.011.

Grenni, P., Ancona, V., & Caracciolo, A. B. (2018). Ecological effects of antibiotics on natural ecosystems:Areview. MicrochemicalJournal, 136,25-39.doi:10.1016/j.microc.2017.02.006.

Ismael, M. (2020). A review on graphitic carbon nitride (g-C3N4) based nanocomposites: synthesis, categories, and their application in photocatalysis. Journal of Alloys and Compounds, 846, 156446. https://doi.org/10.1016/j.jallcom.2020.156446

Kong, Q., He, X., Shu, L., & Miao, M. S. (2017). Ofloxacin adsorption by activated carbon derived from luffa sponge: kinetic, isotherm, and thermodynamic analyses. Process Safety and Environmental Protection, 112, 254-264. https://doi.org/10.1016/j.psep.2017.05.011

Kosmulski, M. (2009). pH-dependent surface charging and points of zero charge. IV. Update and new approach. Journal of colloid and interface science, 337(2), 439-448. https://doi.org/10.1016/j.cis.2017.10.005.

Laverde-Cerda, E., Altamirano-Briones, A., Zárate-Pozo, P., Sandoval-Pauker, C., Ramos-Guerrero, L., Muñoz-Bisesti,

F., & Vargas-Jentzsch, P. (2020). Iron removal for kinetic studies on Fenton treatments: A new approach based on ferrocyanide. Revista Mexicana de Ingeniería Química, 19(1), 159-164. Doi: 10.24275/rmiq/Cat545

Lewis, J. M. T., Eigenbrode, J. L., Wong, G. M., McAdam, A. C., Archer, P. D., Sutter, B., ... & Mahaffy, P. R. (2021). Pyrolysis of oxalate, acetate, and perchlorate mixtures and the implications for organic salts on Mars. Journal of Geophysical Research: Planets, 126(4), e2020JE006803. https://doi.org/10.1029/2020JE006803

Liu, J., Zhang, T., Wang, Z., Dawson, G., & Chen, W. (2011). Simple pyrolysis of urea into graphitic carbon nitride with recyclable adsorption and photocatalytic activity. Journal of Materials Chemistry, 21(38), 14398-14401. doi:10.1039/c1jm12620b

Liu, L., Chen, Z., Zhang, J., Shan, D., Wu, Y., Bai, L., & Wang, B. (2021). Treatment of industrial dye wastewater and pharmaceutical residue wastewater by advanced oxidation processes and its combination with nanocatalysts: A review. Journal of Water Process Engineering, 42, 102122. https://doi.org/10.1016/j.jwpe.2021.102122.

Liu, X., Lu, S., Guo, W., Xi, B., & Wang, W. (2018). Antibiotics in the aquatic environments: a review of lakes, China. Science of the Total Environment, 627, 1195-1208. doi:10.1016/j.scitotenv.2018.01.271.

Ma, Y., Li, M., Wu, M., Li, Z., & Liu, X. (2015). Occurrences and regional distributions of 20 antibiotics in water bodies during groundwater recharge. Science of the Total Environment, 518, 498-506. https://doi.org/10.1016/j.scitotenv.2015.02.100

Manaia, C. M., Rocha, J., Scaccia, N., Marano, R., Radu, E., Biancullo, F., ... & Nunes, O. C. (2018). Antibiotic resistance in wastewater treatment plants: Tackling the black box. Environment international, 115, 312-324. https://doi.org/10.1016/j.envint.2018.03.044.

Michael, I., Rizzo, L., McArdell, C. S., Manaia, C. M., Merlin, C., Schwartz, T., ... & Fatta-Kassinos, D. J. W. R. (2013). Urban wastewater treatment plants as hotspots for the release of antibiotics in the environment: a review. Water research, 47(3), 957-995. https://doi.org/10.1016/j.watres.2012.11.027

Ni, M., & Ratner, B. D. (2008). Differentiating calcium carbonate polymorphs by surface analysis techniques—an XPS and TOF-SIMS study. Surface and Interface Analysis: An International Journal devoted to the development and application of techniques for the analysis of surfaces, interfaces and thin films, 40(10), 1356-1361. https://doi.org/10.1002/sia.2904

Peña-Guzmán, C., Ulloa-Sánchez, S., Mora, K., Helena-Bustos, R., Lopez-Barrera, E., Alvarez, J., & Rodriguez-Pinzón, M. (2019). Emerging pollutants in the urban water cycle in Latin America: A review of the current literature. Journal of environmental management, 237, 408-423. https://doi.org/10.1016/j.jenvman.2019.02.100

Picho-Chillán, G., Dante, R. C., Muñoz-Bisesti, F., Martín-Ramos, P., Chamorro-Posada, P., Vargas-Jentzsch, P., ... & Rutto, D. (2019). Photodegradation of Direct Blue 1 azo dye by polymeric carbon nitride irradiated with accelerated electrons. Materials Chemistry and Physics, 237, 121878. https://doi.org/10.1016/j.matchemphys.2019.121878

Qin, D., Lu, W., Wang, X., Li, N., Chen, X., Zhu, Z., & Chen, W. (2016). Graphitic carbon nitride from burial to re-emergence on polyethylene terephthalate nanofibers as an easily recycled photocatalyst for degrading antibiotics under solar irradiation. ACS Applied Materials & Interfaces, 8(39), 25962-25970. DOI: 10.1021/acsami.6b07680.

Redgrave, L. S., Sutton, S. B., Webber, M. A., & Piddock, L. J. (2014). Fluoroquinolone resistance: mechanisms, impact on bacteria, and role in evolutionary success. Trends in microbiology, 22(8), 438-445. https://doi.org/10.1016/j.tim.2014.04.007.

Sandoval, C., Molina, G., Vargas Jentzsch, P., Perez, J., & Munoz, F. (2017). Photocatalytic degradation of azo dyes over semiconductors supported on polyethylene terephthalate and polystyrene substrates. Journal of Advanced Oxidation Technologies, 20(2), 20170006. https://doi.org/10.1515/jaots-2017-0006

Su, Q., Li, J., Yuan, H., Wang, B., Wang, Y., Li, Y., & Xing, Y. (2022). Visible-light-driven photocatalytic degradation of ofloxacin by g-C3N4/NH2-MIL-88B (Fe) heterostructure: Mechanisms, DFT calculation, degradation pathway and toxicity evolution. Chemical Engineering Journal, 427, 131594.

Su, F., Mathew, S. C., Lipner, G., Fu, X., Antonietti, M., Blechert, S., & Wang, X. (2010). mpg-C3N4-catalyzed selective oxidation of alcohols using O2 and visible light. Journal of the American Chemical Society, 132(46), 16299-16301. https://doi.org/10.1021/ja102866p

Szymańska, U., Wiergowski, M., Sołtyszewski, I., Kuzemko, J., Wiergowska, G., & Woźniak, M. K. (2019). Presence of antibiotics in the aquatic environment in Europe and their analytical monitoring: Recent trends and perspectives. Microchemical Journal, 147, 729-740 https://doi.org/10.1016/j.microc.2019.04.003.

Van Doorslaer, X., Dewulf, J., Van Langenhove, H., & Demeestere, K. (2014). Fluoroquinolone antibiotics: an emerging class of environmental micropollutants. Science of the Total Environment, 500, 250-269.

https://doi.org/10.1016/j.scitotenv.2014.08.075.

Van Wieren, E. M., Seymour, M. D., & Peterson, J. W. (2012). Interaction of the fluoroquinolone antibiotic, ofloxacin, with titanium oxide nanoparticles in water: Adsorption and breakdown. Science of the Total Environment, 441, 1-9. https://doi.org/10.1016/j.scitotenv.2012.09.067.

Wang, H., Li, X., Zhao, X., Li, C., Song, X., Zhang, P., & Huo, P. (2022). A review on heterogeneous photocatalysis for environmental remediation: From semiconductors to modification strategies. *Chinese Journal of Catalysis*, *43*(2), 178-214. https://doi.org/10.1016/S1872-2067(21)63910-4.

Wang, X., Lu, W., Chen, Y., Li, N., Zhu, Z., Wang, G., & Chen, W. (2018). Effective elimination of antibiotics over hot-melt adhesive sheath-core polyester fiber supported graphitic carbon nitride under solar irradiation. Chemical Engineering Journal, 335, 82-93. https://doi.org/10.1016/j.cej.2017.10.061

Wen, J., Xie, J., Chen, X., & Li, X. (2017). A review on g-C3N4-based photocatalysts. Applied surface science, 391, 72-123. https://doi.org/10.1016/j.apsusc.2016.07.030.

Xie, A., Dai, J., Chen, X., He, J., Chang, Z., Yan, Y., & Li, C. (2016). Hierarchical porous carbon materials derived from a waste paper towel with ultrafast and ultrahigh performance for adsorption of tetracycline. RSC advances, 6(77), 72985-72998. DOI: https://doi.org/10.1039/C6RA17286E

Yang, Y., Song, W., Lin, H., Wang, W., Du, L., & Xing, W. (2018). Antibiotics and antibiotic resistance genes in global lakes: a review and meta-analysis. Environment international, 116, 60-73. doi:10.1016/j.envint.2018.04.011.

Yu, Y., Zhu, Z., Fan, W., Liu, Z., Yao, X., Dong, H., ... & Huo, P. (2018). Making of a metal-free graphitic carbon nitride composites based on biomass carbon for efficiency enhanced tetracycline degradation activity. Journal of the Taiwan Institute of Chemical Engineers, 89, 151-161. https://doi.org/10.1016/j.jtice.2018.04.034

Contribución de autores

Autores	Contribución
Iván Cóndor Guevara	Fase Experimental, tabulación, análisis de resultados
Alejandro Altamirano Briones	Fase Experimental, caracterización del material, redacción, análisis de resultados
Katherine Terán	Síntesis del material
Espinoza Isabel	Metodología de laboratorio, redacción
Luis Ramos Guerrero	Formato y Forma, Revisión
Wilson Mamani Aguilar	Revisión, refuerzo a resultados
Christian Sandoval Pauker	Revisión, refuerzo a resultados
Paul Vargas Jentzsch,	Dirección del trabajo y revisión de resultados
Florinella Muñoz Bisesti	Revisión, refuerzo a resultados